Acta Oceanol. Sin., 2018, Vol. 37, No. 7, P. 118–130
DOI: 10.1007/s13131-018-1249-6
http://www.hyxb.org.cn
E-mail: hyxbe@263.net

A new merged dataset of global ocean chlorophyll *a* concentration with higher spatial and temporal coverage

XIAO Yanfang[1]*, ZHANG Jie[1], CUI Tingwei[1], SUN Ling[2]

[1] The First Institute of Oceanography, State Oceanic Administration, Qingdao 266061, China

[2] National Satellite Meteorological Center, Key Laboratory of Radiometric Calibration and Validation for Environmental Satellites, China Meteorological Administration, Beijing 100081, China

Received 27 September 2017; accepted 20 October 2017

Abstract

Understanding the ocean's role in the global carbon cycle and its response to environmental change requires a high spatio-temporal resolution of observation. Merging ocean color data from multiple sources is an effective way to alleviate the limitation of individual ocean color sensors (e.g., swath width and gaps, cloudy or rainy weather, and sun glint) and to improve the temporal and spatial coverage. Since the missions of Sea-Viewing Wide Field-of-View Sensor (SeaWiFS) and Medium-spectral Resolution Imaging Spectrometer (MERIS) ended on December 11, 2010 and May 9, 2012, respectively, the number of available ocean color sensors has declined, reducing the benefits of the merged ocean color data with respect to the spatial and temporal coverage. In present work, Medium Resolution Spectral Imager (MERSI)/FY-3 of China is added in merged processing and a new dataset of global ocean chlorophyll *a* (Chl *a*) concentration (2000–2015) is generated from the remote sensing reflectance (Rrs (λ)) observations of MERIS, Moderate-resolution imaging spectra-radiometer (MODIS)-AQUA, Visible infrared Imaging Radiometer (VIIRS) and MERSI. These data resources are first merged into unified remote sensing reflectance data, and then Chl *a* concentration data are inversed using the combined Chl *a* algorithm of color index-based algorithm (CIA) and OC3. The merged data products show major improvements in spatial and temporal coverage from the addition of MERSI. The average daily coverage of merged products is approximately 24% of the global ocean and increases by approximately 9% when MERSI data are added in the merging process. Sampling frequency (temporal coverage) is greatly improved by combining MERSI data, with the median sampling frequency increasing from 15.6% (57 d/a) to 29.9% (109 d/a). The merged Chl *a* products herein were validated by *in situ* measurements and comparing them with the merged products using the same approach except for omitting MERSI and GlobColour and MEaSUREs merged data. Correlation and relative error between the new merged Chl *a* products and *in situ* observation are stable relative to the results of the merged products without the addition of MERSI. Time series of the Chl *a* concentration anomalies are similar to the merged products without adding MERSI and single sensors. The new merged products agree within approximately 10% of the merged Chl *a* product from GlobColour and MEaSUREs.

Key words: merged data, ocean color, chlorophyll *a*, CIA, FY-3 MERSI, VIIRS

Citation: Xiao Yanfang, Zhang Jie, Cui Tingwei, Sun Ling. 2018. A new merged dataset of global ocean chlorophyll *a* concentration with higher spatial and temporal coverage. Acta Oceanologica Sinica, 37(7): 118–130, doi: 10.1007/s13131-018-1249-6

1 Introduction

With the advantages of large-scale and high-frequency repeated observation, ocean color remote sensing is irreplaceable in research into global climate change, biogeochemical cycles, marine dynamics and biological processes, and fisheries (Platt and Sathyendranath, 1988; Arrigo et al., 2008; Murtugudde et al., 2002; Kara et al., 2004; Liang and Wu, 2013). Since 1997, several global satellite sensors, such as GeoEye's Sea-Viewing Wide Field-of-View Sensor (SeaWiFS), NASA's MODIS on the TERRA and AQUA platforms, ESA's Medium-spectral Resolution Imaging Spectrometer (MERIS) on Envisat, NASA's Visible infrared Imaging Radiometer (VIIRS) on the NPP platform, ESA's OLCI on Sentinel-3 and others, have orbited the earth and provided vast amounts of ocean color data (McClain, 2009). However, an individual ocean color sensor is limited in daily ocean coverage because of its swath width and gaps, cloudy or rainy weather, and sun glint (Maritorena and Siegel, 2005; Gregg et al., 1998; Pottier et al., 2006; Loeb et al., 2009).

The challenge of understanding the ocean's role in the global carbon cycle and its response to environmental change requires enlargement of observation scale in both space and time (Johnson et al., 2009; Chavez et al., 2011). Merging datasets from different missions into unified data products are a valid way to increase the spatial and temporal coverage of ocean color satellites (Gregg et al., 1998; Gregg and Woodward, 1998; Maritorena and Siegel, 2005). Furthermore, the merged products can also mitigate confusion, because data users are sometimes unsure as to which ocean color dataset to use when several satellite missions cover the same region. Within the NASA SIMBIOS, REASoN and MEaSUREs projects or ESA's GlobColour and OC_CCI programs,

Foundation item: The National Key R & D Program of China under contract No. 2016YFA0600102; the National Natural Science Foundation of China under contract Nos 41506203, 41476159, 41506204, 41606197, 41471303 and 41706209; the Cooperation Project of FIO and KOIST under contract No. PI-2017-03.

*Corresponding author, E-mail: xiaoyanfang@fio.org.cn

Table 1. Summary of principal characteristics of currently available merged ocean color datasets

Datasets	Temporal/spatial resolution	Input data	Time	Merging method
GlobColour project (ESA)	daily, 8-day, monthly/4.5 km, (1/4)°, 1°	MERIS, MODIS-AQUA, SeaWiFS, VIIRS	1997–now	GSM01 model weighted average
OC_CCI project (ESA)	daily, 8-day, monthly/4.5 km	MERIS, MODIS-AQUA, SeaWiFS	1997–2012	weighted average (with band shifting)
MEaSUREs (NASA)	daily, 4-day, 8-day, monthly/9 km	MERIS, MODIS-AQUA, SeaWiFS	2002–2010	GSM01 model

there have been several data merging efforts for ocean color in recent years (Table 1) (Gregg and Conkright, 2001; Kwiatkowska and Fargion, 2002; Maritorena and Siegel, 2005; Pottier et al., 2006; IOCCG, 2007; Mélin et al., 2009; Maritorena et al., 2010; Kahru et al., 2015). Final merged ocean color data products are generated by compositing ocean color observations from various missions into a single dataset (Kwiatkowska and Fargion, 2003a, 2003b; Saulquin et al., 2011), or by inputting water-leaving radiance from those missions into a bio-optical model to inverse ocean color merged data (Garver and Siegel, 1997; Maritorena et al., 2002, 2010; Maritorena and Siegel, 2005). Both approaches have been used and the merged datasets are now available to the scientific community and researchers (Kahru et al., 2012; Ford and Barciela, 2017).

The main data sources for the available merged ocean color datasets generated by NASA and ESA are Moderate-resolution imaging spectra-radiometer (MODIS)-AQUA, SeaWiFS, MERIS, and VIIRS. SeaWiFS stopped collecting data on December 11, 2010, and MERIS stopped working on May 9, 2012. MODIS has exceeded its projected lifespan and could fail at any time. VIIRS onboard the SNPP spacecraft was launched on October 28, 2011, with swath width approximately 3 000 km. ESA launched the Sentinel-3A satellite on February 16, 2016 and its OLCI instrument gives continuity for the MERIS instrument capability, but it will provide ocean color product service for a period (Donlon et al., 2012). A report from the US National Academies Press states that remote sensing capabilities and data continuity are degrading, and this is particularly serious for ocean color data. This gives a high probability of research-quality data gaps in the future (Siegel and Yoder, 2007; Turpie, 2010). The reduction of data sources for merging will reduce the benefits of merged data with regard to spatial and temporal coverage.

The Fengyun-3 (FY-3) is the second generation of China's polar-orbiting meteorological weather satellite series, and includes four spacecraft (FY-3A, FY-3B, FY-3C and FY-3D). They were launched on May 27, 2008, November 5, 2010, September 23, 2013 and November 15, 2017, respectively. The Medium Resolution Spectral Imager (MERSI) carried during these missions is a MODIS-like sensor with 20 bands covering the visible, near-infrared, shortwave infrared, and thermal infrared spectral regions. Nine bands can be used for ocean color monitoring with swath width of 2 900 km and nadir spatial resolution of 1 km. FY-3 MERSI has the capability of collecting continuous global observation data for a range of scientific studies of the earth system, including ocean color application (Sun et al., 2012), and may be an important potential data source for the merging of ocean color data.

The main purpose of this paper is to introduce a new merged global ocean Chlorophyll *a* (Chl *a*) concentration dataset from 2000 to 2015 combining the frequently-used sensors MODIS, MERIS, SeaWiFS and VIIRS and the potential sensor FY-3 MERSI from normalized water-leaving reflectance observations with 9-km spatial resolution. This paper establishes upon existing merged sensor products of ocean color by incorporating data from the FY-3 MERSI sensor. The methods for MERSI data modification and integration are described with reference to existing processing chains. The resulting improvements in spatio-temporal coverage are quantified and the product validation is provided through the use of *in situ* data and comparison with existing merged data products. The implications and limitations of the approach are discussed in the context of climate quality data records. Chl aorophyll

2 Data and method

2.1 *Data*

To produce the merged time-series global ocean Chl *a* concentration products, daily level-3 remote sensing reflectance (Rrs) data products (≈9 km) of MERIS, MODIS-Aqua and VIIRS were downloaded from the NASA ocean-color website (http://oceancolor. gsfc.nasa.gov, processing Version 2014.0) for the period of 2011– 2014. These data were processed using SeaDAS (Gregg et al., 2002; Antoine et al., 2005; Morel et al., 2007; Mélin et al., 2011).

MERSI in FY-3 series satellites is a cross-track scanning radiometer using a 45° scan mirror, and makes earth view observations through a ±55° scan angle about the nadir. The collected data have two nadir spatial resolutions: 250 m (five bands) and 1 000 m (15 bands). The swath is 2 900 km, enabling complete global coverage in one day. Although MERSI has a visible/near infrared(VIR/NIR) onboard calibrator, the experimental device is only used for tracking temporal degradation of the instrument for research purposes, because of its irregular operation and inability to be traced back to the pre-launch standard (Sun et al., 2012). The baseline calibration of MERSI is the vicarious calibration using synchronous *in situ* measurements at China's radiometric calibration site (CRCS) at Dunhuang Gobi Desert every summer (Hu et al., 2010), and a daily update procedure based on multisite calibration is used for reprocessing (Sun et al., 2012). The daily level-3 Rrs data (≈5 km) of FY-3 MERSI, with atmospheric correction by algorithms similar to MODIS (Sun et al., 2013), were obtained from the National Satellite Meteorological Center of the China Meteorological Administration.

2.2 *Merging method*

The present merging procedure is shown in Fig. 1 and its main components are briefly summarized below. One of the major features of the procedure is that the combination begins with Rrs data products from different sensors, and another is that Chl *a* concentration data are inversed using the combined algorithm of color index-based algorithm (CIA) and OC3. The latter two are default algorithm formulations to produce global Chl *a* concentration products. The MERIS, MODIS, SeaWiFS and VIIRS missions have been widely evaluated and compared, and all have good-quality Rrs data (Hooker and Maritorena, 2000; McClain et al., 2002; Kwiatkowska, 2003; Franz, 2003; Bailey and Werdell, 2006; Antoine et al., 2008; Hu et al., 2013; Hlaing et al., 2013). We combined Rrs data from these four missions into unified Rrs data

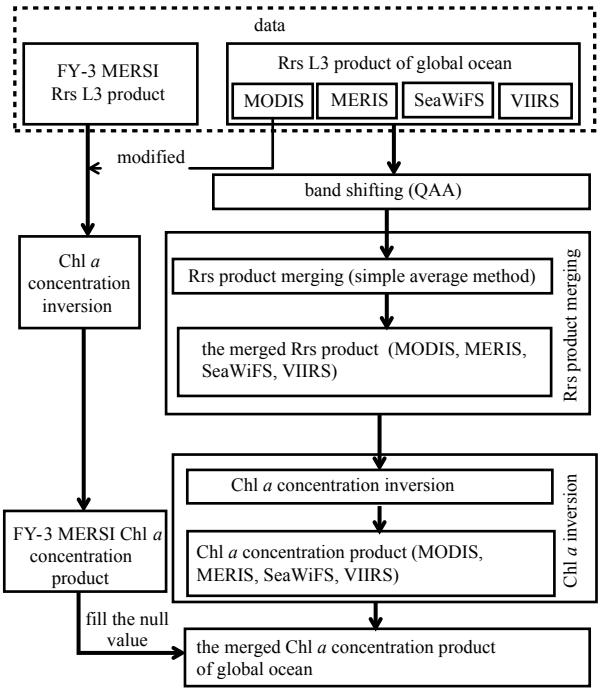

Fig. 1. Schematic of merging method used. Rrs is abbreviated from Rrs.

after shifting the MODIS, MERIS and VIIRS bands into SeaWiFS bands, which overcame the problem of different sensor band settings (Zibordi et al., 2006, 2009; Antoine et al., 2008; Mélin et al., 2011). For FY-3 MERSI data, the consistency of Rrs products from MODIS were analyzed, and the FY-3 Rrs products were corrected according to the relationship between the two Rrs products. Then, the Chl *a* concentration data were inversed using the same algorithm, and Chl *a* concentration values were used at invalid pixels of the Chl *a* concentration products merged by MODIS, MERIS, SeaWiFS and VIIRS. This produced the final global ocean Chl *a* concentration products.

Correcting for differences in wavebands of different missions is required for intercomparison and as a pre-processing step before merging (Zibordi et al., 2006, 2009; Antoine et al., 2008; Mélin and Zibordi, 2007; Mélin et al., 2009, 2011). The band-shift correction approach adopted herein is described in detail in the product user guide of ESA's OC_CCI program (http://www.esa-oceancolour-cci.org/?q=documents). Here, MODIS, MERIS and VIIRS were band-shifted to the five main SeaWiFS bands (center wavelengths 412, 443, 490, 555 and 670 nm) by computing QAA IOPs (Lee et al., 2002, 2010) and back-computing Rrs bands using a high-resolution spectral model. Table 2 shows the wavelength sets for MODIS, MERIS, SeaWiFS and VIIRS. The 510 nm band was not included in the merged Rrs data because MODIS lacks it, and this is why the OC4 algorithm was not used in our combined Chl *a* concentration inversion algorithms.

Differences in Rrs data from various sensors can be caused by either a lack of synopticity or other issues associated with algorithms, calibrations and other sensor characteristics (e.g., band setting, solar diffuser, sensitivity to polarization) (Fargion and McClain, 2003; Maritorena and Siegel, 2005). To analyze the effectiveness of band shifting, simulated observations of Rrs were used to avoid noise sources other than the band setting. The radiative transfer model Hydrolight (Mobley, 1994; Mobley and Sundman, 2013; Lee et al., 2015) was used to generate the Rrs spectrum of case-1 water for MODIS, SeaWiFS, MERIS and VIIRS from a range of Chl *a* concentration values (0.03–3.00 mg/m^3). We analyzed consistency between the Rrs values of MODIS, MERIS and VIIRS after band shifting and Rrs values of SeaWiFS. This assessment was done by comparing relative error between the original or band-shifted Rrs values from MODIS, MERIS and VIIRS bands and Rrs values from corresponding bands of SeaWiFS (Table 3). Fargion and McClain (2003) compared the consistency of water-leaving radiance between SeaWiFS and MODIS Terra, and daily mean percentage differences in corresponding bands (nLw_412 and nLw_443) were greater than 5%. The small relative error of Rrs in 412 nm and 443 nm in Table 3 shows that the use of simulated data can remove noise caused by algorithms, calibrations and other sensor characteristics (e.g., band setting, solar diffuser, sensitivity to polarization). For most bands, the band shift improves agreement between Rrs values. The greatest change was for the green band. For the MODIS green band, the relative error decreased from 9.58% to 2.89% after MODIS Rrs at 547 nm was shifted to that at 555 nm. For the MERIS green band, relative error decreased from 4.44% to 0.91% after the MERIS Rrs at 560 nm was shifted to that at 555 nm. The improvement from band shifting was obvious, and demonstrated how data with similar accuracy but different band set-

Table 2. Wavelength sets for SeaWiFS, MODIS, MERIS and VIIRS (in nm)

Sensors	Bands					
SeaWiFS	412	443	490	510	555	670
MERIS	413	443	490	510	560	667
MODIS	412	443	488	531	547	665
VIIRS	410	443	486	–	551	671
merged	412	443	490	–	555	670

Table 3. Consistency between Rrs in principal bands of MODIS, MERIS and VIIRS after band shifting and Rrs SeaWiFS

MODIS		MERIS		VIIRS		SeaWiFS		Relative error of MODIS/%	Relative error of MERIS/%	Relative error of VIIRS/%
λ/nm	Rrs/10^{-3}	λ/nm	Rrs/10^{-3}	λ/nm	Rrs/10^{-3}	λ/nm	Rrs/10^{-3}			
412	9.029	413	8.984	410	9.026	412	8.886	1.609	1.103	1.576
				412*	8.837					0.551
443	6.882	443	6.870	443	6.808	443	6.832	0.732	0.556	
488	5.666	490	5.543	486	5.629	490	5.410	4.732	2.458	4.048
490*	5.590			490*	5.546			3.327		2.514
547	2.538	560	2.213	551	2.467	555	2.316	9.586	4.447	6.520
555*	2.249	555*	2.337	555*	2.391			2.893	0.907	3.238
665	0.245	667	0.248	671	0.261	670	0.240	2.083	3.333	
670*	0.233	670*	0.242					2.917	0.833	

Note: * means that the band was shifted.

tings can be efficiently used in data merging.

The band shift decreased means and standard deviations of relative error for most bands of MODIS, MERIS and VIIRS (Fig. 2). However, for MODIS Rrs at 531 nm, the absolute average percent deviation (APD) remained approximately 10% after shifting to the Rrs value at 510 nm, and the standard deviation was not reduced much. The effect of band shifting was more obvious for MERIS than for MODIS and VIIRS, which may have been a result of differences of passing time.

The Chl *a* concentration inversion algorithm used is a combination of the color index-based algorithm (CIA) (Hu et al., 2012) and OC3 (NASA, 2010). The CIA is a new empirical algorithm proposed by Hu et al. (2012) to estimate surface Chl *a* concentrations in the global ocean for Chl *a* concentration being less than 0.15 mg/m^3. The algorithm is based on a color index (CI), which is defined as the difference between Rrs in the green and a reference formed linearly between Rrs in the blue and red bands. For larger Chl *a* values (> 0.2 mg/m^3), the standard band-ratio algorithm OC3 was adopted. For intermediate Chl *a* concentrations (0.15 mg/m^3 < *c*(Chl *a*) < 0.2 mg/m^3), a mixture between the two algorithms was used to ensure image smoothness when the algorithm switches from one to the other. Detailed information on the CIA is found in Hu et al. (2012).

3 Assessment and correction of FY-3 MERSI Rrs data

For the merging data from different ocean color sensors, it is necessary to verify that the products for merger are consistent within their own uncertainty levels. Because of the differences in spatial resolution between MODIS and FY-3 MERSI data, grids of FY-3 MERSI data were first resampled to 9 km by averaging. Then, each grid of FY-3 MERSI data was matched with MODIS data. This process was done between FY-3 MERSI Rrs daily data of 2011 for the 412, 443, 490, 565 and 650 nm bands, and MODIS Rrs daily data of the same year for the 412, 443, 488, 555 and 667 nm bands, respectively. In this procedure, we did not consider the waveband differences between the two instruments.

Statistical measures of consistency between MODIS and FY-3 MERSI Rrs data are listed in Table 4. Note that when evaluating the relative difference between two datasets *x* and *y* (in this case, *x* is the Rrs value of MODIS, and *y* is that value of FY-3 MERSI), APD_median is the median value with form $|(y\text{-}x)/y|$, and bias is typically evaluated using the form *y*-*x*. The results show a weak relationship between MODIS and FY-3 MERSI Rrs(λ) data, with small correlation coefficients *r* (0.370–0.570 for FY-3A and 0.547–0.806 for FY-3B) and large APD_median differences (57.7%–1 375% for FY-3A and 52.8%–2 208% for FY-3B).

Figure 3 displays frequency distributions of Rrs values from MODIS and FY-3A MERSI. These values from the two instruments all have a near-normal distribution, but the peaks are different (except 412 nm). Compared with MODIS, the Rrs value ranges of FY-3A MERSI are wider and the magnitudes are larger for most bands.

MODIS and FY-3 MERSI use similar atmospheric correction framework, so calibration algorithms and sensor performance are the main causes of the large variation between Rrs data of the two instruments, the cloud mask performance is also a possible reason. The contributions of the origins of Rrs error are outside the scope of the present study. The primary objective was to consider if it is possible to obtain the Chl *a* concentration products from FY-3 MERSI Rrs data, which are consistent with MODIS Chl *a* concentration products within acceptable levels, under the condition of large difference between the two Rrs datasets.

Three indices used in the Chl *a* concentration inversion algorithm, Rrs (443)/ Rrs (565), Rrs (490)/ Rrs (565) and CI of FY-3 MERSI, are compared with MODIS in Table 5. This shows considerable improvement in the consistency of the three indices between MODIS and FY-3 MERSI as compared with Rrs observations, with larger correlation coefficient (0.847–0.922 for FY-3A and 0.822–0.912 for FY-3B) and smaller APD_median difference (23.91%–170% for FY-3A, and 25.6%–355% for FY-3B). Figure 4 displays scatter plots and frequency distributions of Rrs (443)/ Rrs (565), Rrs (490)/ Rrs (565) and CI between MODIS and FY-3A MERSI. It shows that the difference between the two instruments is mainly caused by systematic bias, which can be corrected by certain functions. The three indices of FY-3A MERSI have similar shapes of the frequency distribution curve with MODIS data, al-

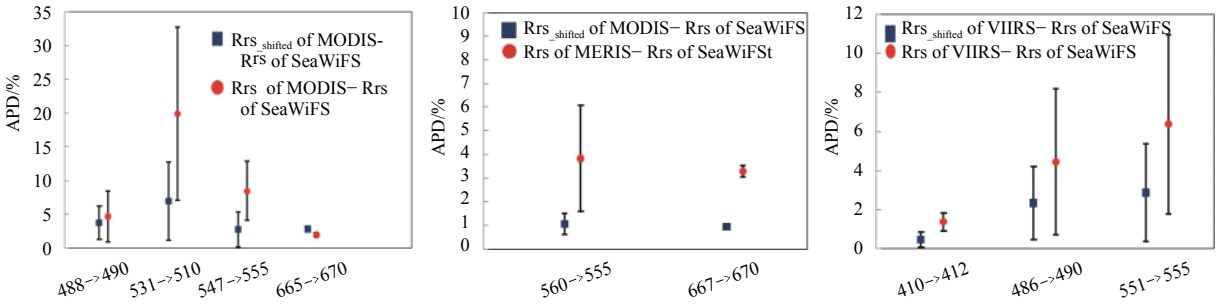

Fig. 2. The means and standard deviations of the absolute average percent deviation for MODIS (left), MERIS (middle), and VIIRS (right) band shifts. Red circles show results before band shifting and blue squares those after band shifting.

Table 4. Consistency between MODIS and FY-3 MERSI Rrs data

λ/nm	FY-3A & MODIS				FY-3B & MODIS			
	r	RMSE/sr^{-1}	bias/sr^{-1}	APD-median/%	*r*	RMSE/Sr^{-1}	bias/Sr^{-1}	APD-median/%
412	0.452	0.010	0.005	57.7	0.589	0.009	–0.007	52.8
443	0.487	0.032	0.030	430	0.806	0.027	0.025	369
490	0.370	0.034	0.033	599	0.580	0.041	0.045	787
565	0.557	0.018	0.017	814	0.547	0.021	0.021	993
650	0.570	0.005	0.003	1 375	0.578	0.006	0.005	2 208

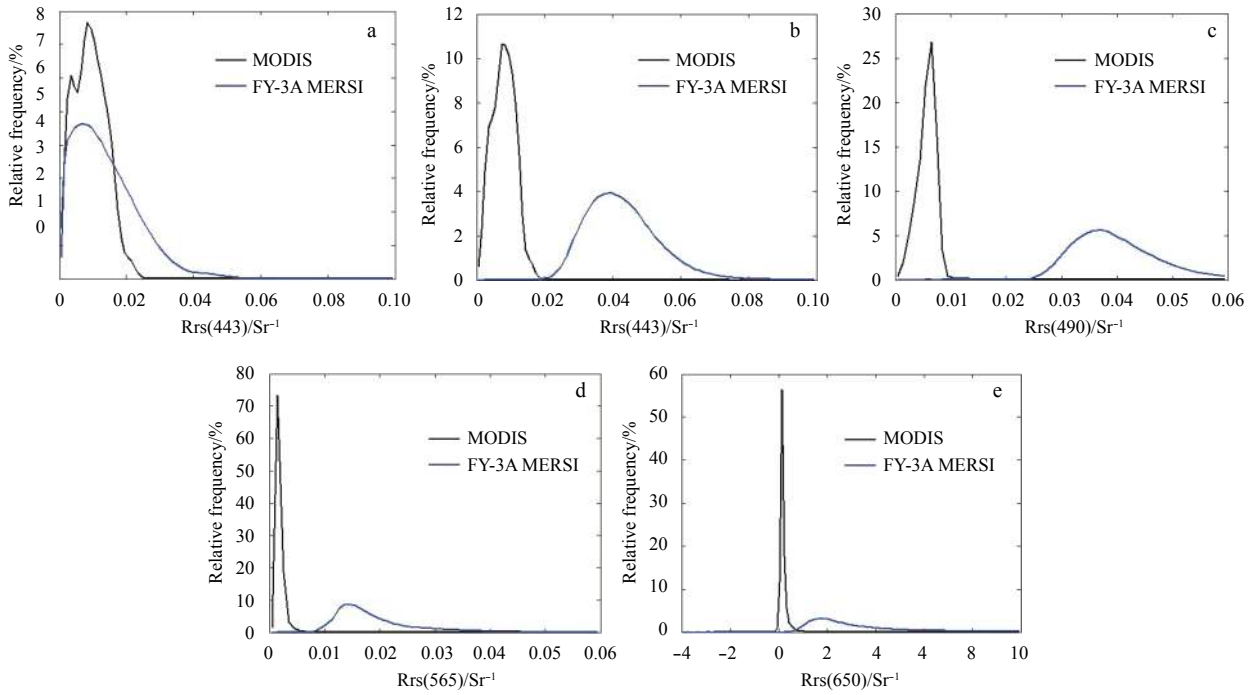

Fig. 3. Frequency distribution of remote sensing reflectance values of 412 nm for FY-3A MERSI and MODIS (a), 443 nm for FY-3A MERSI and MODIS (b), 488 nm for FY-3A MERSI and 490 nm for MODIS (c), 565 nm for FY-3A MERSI and 555 nm for MODIS (d), and 650 nm for FY-3A MERSI and 667 nm for MODIS (e).

Table 5. Consistencies of Rrs (443)/Rrs (565), Rrs (490)/Rrs (565) and CI indices between FY-3 MERSI and MODIS

	FY-3A and MODIS				FY-3B and MODIS			
	r	RMSE/sr^{-1}	Bias/sr^{-1}	APD-median/%	*r*	RMSE/sr^{-1}	Bias/sr^{-1}	APD-median/%
*R*rs(443)/*R*rs(565)	0.906	2.07	–1.46	40.51	0.873	1.99	–1.30	54.01
*R*rs(490)/*R*rs(565)	0.847	0.89	–0.535	23.91	0.822	1.22	–0.918	25.60
CI	0.922	0.005	-1.33×10^{-5}	170.35	0.912	0.0075	-7.30×10^{-4}	355.37

though the value ranges of those indices of the two missions still have some differences. The results illustrate that it is possible to obtain the available Chl *a* concentration from FY-3 MERSI Rrs data by correcting the three indices using MODIS data.

The Chl *a* concentration products were obtained from FY-3 MERSI Rrs data using the inversion approach proposed by Hu et al. (2012), after Rrs(443)/ Rrs(565), Rrs(490)/ Rrs(565) and CI were corrected using MODIS data. The products were compared with the Chl *a* concentration products of MODIS, which were re-created from Rrs data using the same inversion method. Statistical measures of consistency are listed in Table 6. There is satisfactory agreement between FY-3 and MODIS Chl *a* concentration products. An example of geographic and frequency distributions of the FY-3 MERSI and MODIS Chl *a* concentration products is displayed in Fig. 5. It shows similar distributions between the two products over most of the global ocean. Peaks of the histograms are both around Chl *a* concentration 0.2 mg/m^3, close to the mean value (0.193 mg/m^3) (Wang, 2005) for deep oceanic waters. Substantial discrepancies appear in coastal waters, where the Chl *a* returns from FY-3 MERSI were systematically weaker than those from MODIS. Because of the complicated variability of optical properties in coastal waters, the performance of any algorithm is generally degraded (Le et al., 2013). The considerable discrepancy of Chl *a* concentration returns in coastal waters also exists among the products of MODIS, MERIS and SeaWiFS.

4 Results and discussion

4.1 *Example of new merged Chl a concentration data products*

Figure 6 shows an example of daily images for Chl *a* products of March 22, 2011 from MODIS AQUA (Fig. 6a), MERIS (Fig. 6b), FY-3A (Fig. 6c), FY-3B (Fig. 6d), and daily Chl *a* merged products (Fig. 6e). Panels a, b, c and d show differences in daily available coverage between the four sensors. The merged Chl *a* image (Panel e) from Rrs data of the four sensors does not show any obvious artifacts, except in coastal waters where algorithms are not expected to provide accurate results. Compared with the individual sensors, the merged image shows strong improvement in daily coverage.

The average contributions of the individual sensors to daily coverage of merged data were calculated for 2011 and 2013. The Chl *a* concentration products of 2011 were merged from the Rrs data of MERIS, MODIS AQUA, FY-3A and FY-3B. Of the valid bins of merged data, 24.2% (standard deviation 4.6%) were from MODIS AQUA-only data, 28.7% (standard deviation 5.2%) from MERIS-only data, 9.6% (standard deviation 2.5%) from the combination of MODIS AQUA and MERIS, and 37.5% (standard deviation 7.3%) from FY-3-only data (FY-3A and FY-3B were available in 2011). The Chl *a* concentration products of 2013 were merged from the Rrs data of MODIS AQUA, VIIRS and FY-3B. Of the valid bins of merged data, 23.3% (standard deviation 4.0%) were from MODIS AQUA-only data, 23.1% (standard deviation

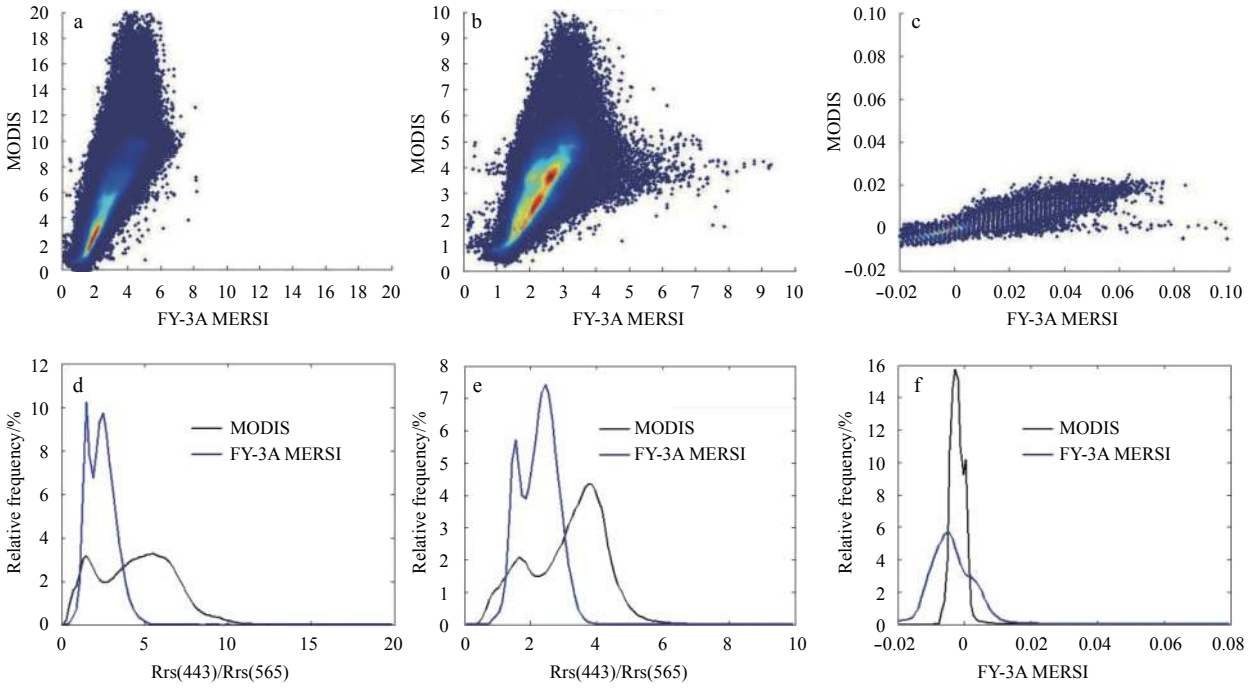

Fig. 4. Scatter plots and frequency distributions of Rrs (443)/Rrs(565), Rrs (490)/Rrs (565) and CI between MODIS and FY-3A MERSI. a–c. Density scatter plots of Rrs (443)/Rrs (565), Rrs (490)/Rrs (565) and CI indices between FY-3A MERSI and MODIS. Warm colors indicate a high density of matching and cool colors a low density. d–f. Corresponding frequency distributions of three indices of FY-3A MERSI and MODIS.

Table 6. Consistencies of monthly Chl *a* concentration products between FY-3 MERSI and MODIS for 2011

	*r**	RMSE*	bias*	APD-median/%*
FY-3A vs. MODIS	0.92	0.21	0.069	14.11
FY-3B vs. MODIS	0.89	0.22	0.074	15.09

Note: * means that the statistical measures are made based on the logarithm of Chl *a* concentration value.

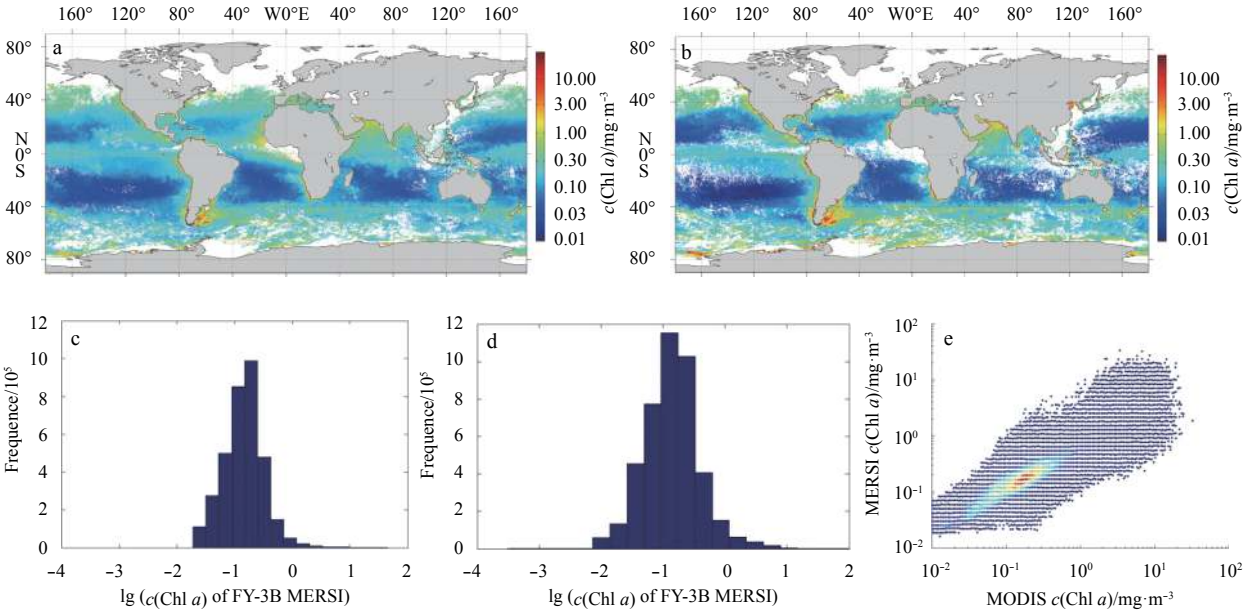

Fig. 5. Example Chl *a* concentration product of FY-3B MERSI and MODIS for January 2011. a. Geographic distribution of Chl *a* concentration for FY-3B MERSI, produced by inversion algorithm proposed by Hu et al. (2012); b. geographic distribution of Chl *a* concentration for MODIS, produced by same inversion algorithm; c and d corresponding frequency histograms for FY-3B MERSI and MODIS Chl *a* concentration products; the e. scatter density diagram between modified FY-3B MERSI Chl *a* concentration product and MODIS Chl *a* concentration product.

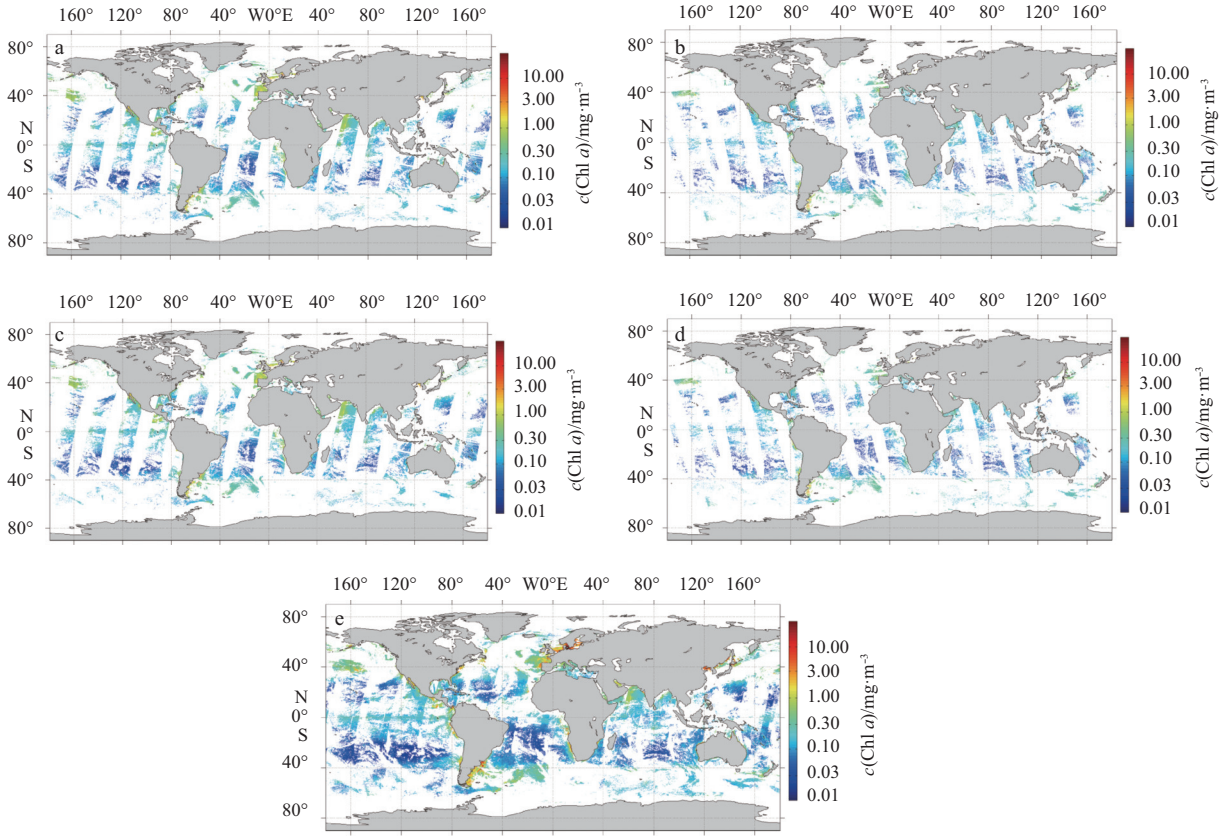

Fig. 6. Daily maps (March 22, 2011) of Chl *a* concentration from MODIS AQUA (a), MERIS (b), FY-3A (c), FY-3B (d) and daily Chl *a* merged products from the four sensors (e).

4.1%) from VIIRS-only data, 29.4% (standard deviation 5.6%) from the combination of MODIS AQUA and VIIRS, and 24.2% (standard deviation 3.5%) from FY-3-only data (only FY-3B was available in 2013).

4.2 *Benefits to spatial and temporal coverage*

4.2.1 *Spatial coverage*

Increasing daily spatial coverage of the global ocean is the most obvious benefit of merging multiple sensors (Gregg et al., 1998; Maritorena and Siegel, 2005; Pottier et al., 2006; Mélin et al., 2009; Maritorena et al., 2010). The spatial coverage increases with the number of sensors. Figure 7 shows examples of daily Chl *a* merged products with and without adding FY-3 MERSI, using the same Chl *a* concentration inversion algorithm for January 1, 2011. SeaWiFS data were not incorporated in the merged images, because it stopped acquiring data on December 11, 2010. Daily coverage of the merged images jumped from 13.6% (Fig. 7a) of the global ocean surface to 24.6% (Fig. 7b) with use of FY-3 MERSI in the merger.

Table 7 shows average daily global coverage for 2010–2013 of SeaWiFS, MODIS, MERIS, VIIRS, FY-3 MERSI and the merged products, with and without FY-3. Each individual sensor covers about 6.00%–14.00% of the global ocean daily on average (SeaWiFS: 6.25% for 2010; MODIS: 8.00% for 2010–2013; MERIS: about 6.50%–10.00% for 2010–2012; VIIRS: 8.00% for 2012–2013; FY-3: 11.70%–14.00% for 2010–2013). When the sensors are combined except for FY-3 MERSI, the daily coverage increases to 11.50% (combination of MODIS and VIIRS) and 16.50% (combination of SeaWiFS, MODIS and MERIS). If FY-3 MERSI is included in the merged products, the coverage clearly improves. The increase in coverage is approximately 9.00% when FY-3A and FY-3B are both added in the merger, and approximately 4.50% when only one is added. The improved daily coverage allows complete coverage of the global ocean in a shorter time, which would be very useful to study ocean processes at high temporal resolution

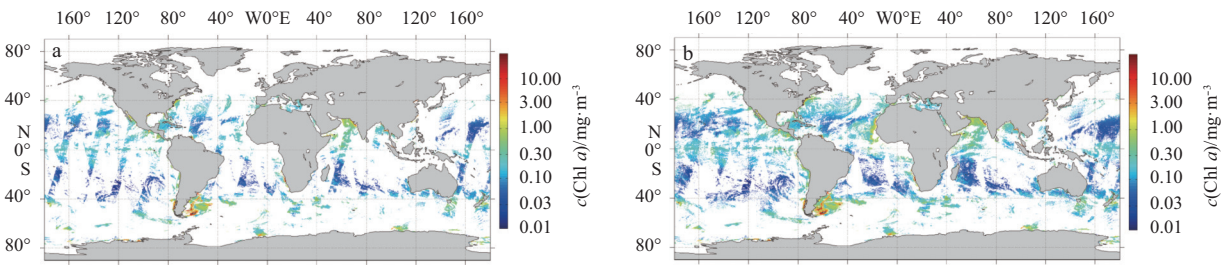

Fig. 7. Daily merged Chl *a* maps (January 1, 2011) from MODIS and MERIS (a), and from MODIS, MERIS and FY-3 MERSI (b).

Table 7. Average daily coverage of individual sensors and merged products (2010–2013)

Year	Individual sensor						Merged product	
	SeaWiFS	MODIS	MERIS	VIIRS	MERSI/FY-3A	MERSI/FY-3B	No-adding FY-3	Adding FY-3
2010	6.25%	8.39%	10.15%				16.46%	16.72%
2011		8.47%	9.72%		14.45%	11.69%	14.78%	24.06%
2012		8.49%	6.56%	8.29%		13.13%	11.95%	16.63%
2013		8.56%		8.54%		12.57%	11.49%	15.09%

(Maritorena, 2005).

4.2.2 *Temporal coverage*

Aside from the benefit in surface area coverage, another important improvement of data merger is temporal coverage, i.e., sampling frequency. Figure 8 shows this increased frequency for the global ocean, with and without FY-3 MERSI addition to the merged Chl *a* products. Note that the temporal coverage is expressed in number of days of valid observations each year over the period January 2011–December 2013. The general distribution of temporal coverage shows some differences between the oceans. For the merged products without FY-3 MERSI, the central Pacific, central Atlantic, central Indian Ocean, west coasts of North America, South Africa and Mediterranean Sea, and Australian coasts have the most frequent coverage. For the merged products with FY-3 MERSI, mid and low latitudes (40°S–40°N) are highly sampled, except for equatorial regions of the Pacific and Atlantic, west coasts of Africa and South America, and marginal seas of the western North Pacific. Conversely, high latitudes (>50°) have much less sampling frequency for the merged products.

For 2011, the merged products without FY-3 MERSI have combined MODIS and MERIS. The median sampling frequency is 15.60%, equivalent to 57 d/a on average. Maximum sampling frequency is 70.00% (256 d/a). Only 0.10% of the global ocean bins have data more than 50.00% of the time (183 d/a), and bins having data more than 30% (110 d/a) make up 11.30%. The merged products with FY-3 MERSI have much better temporal coverage, with the median increasing to 29.90% (109 d/a) and maximum to 87.70% (320 d/a). About 15.50% of the bins have data more than 50.00% of the time (183 d/a). For 2012 and 2013, the merged products without FY-3 MERSI were mainly generated by MODIS and VIIRS. The sampling frequency is similar to the data of 2011. The median sampling frequency is 12.00% (44 d/a) and the area with most frequent sampling has data 75.00% of the time (275 d/a). Bins with data more than 50.00% of the time

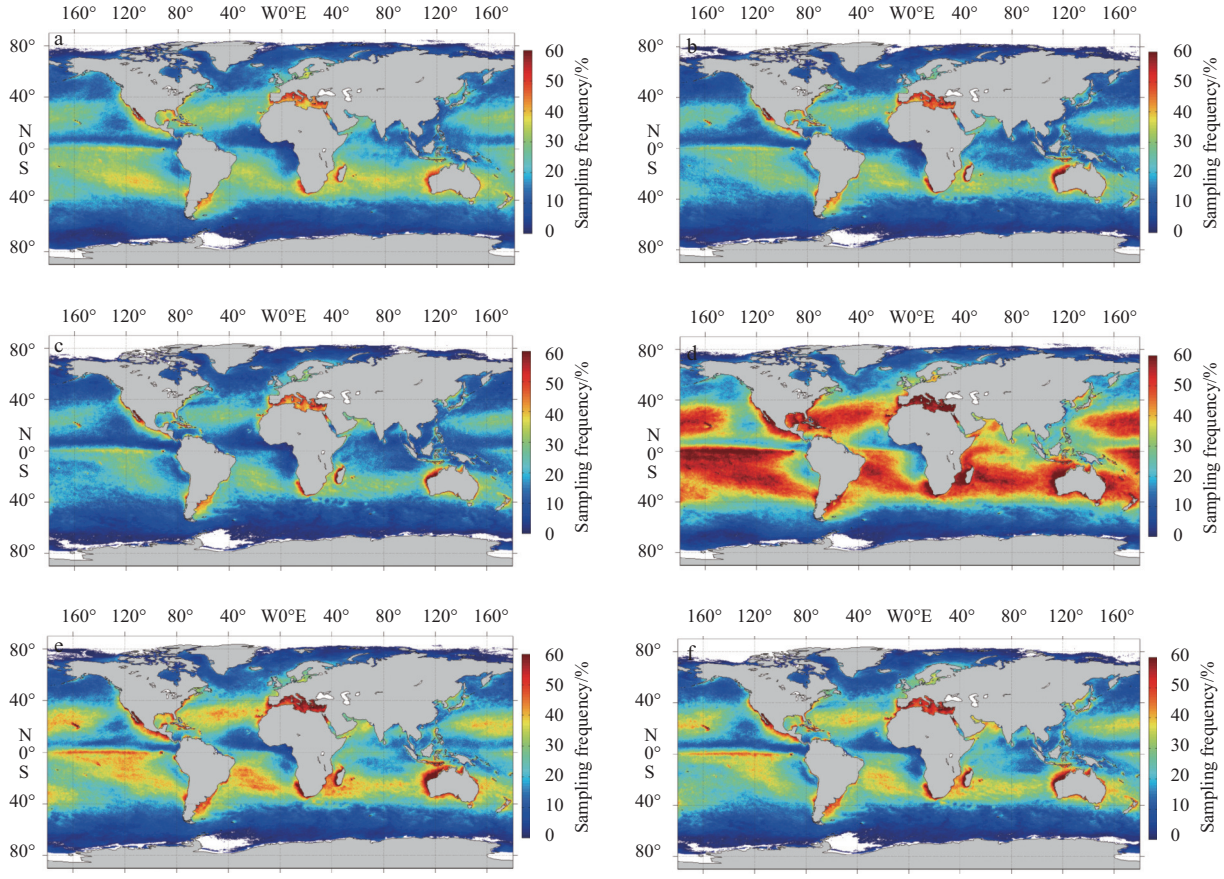

Fig. 8. Geographic distribution of sampling frequency for merged Chl *a* products combining MODIS and MERIS (2011) (a), MODIS and VIIRS (2012) (b), MODIS and VIIRS (2013) (c), MODIS, MERIS, FY-3A and FY-3B MERSI (2011) (d), MODIS, VIIRS, and FY-3B (e), MODIS, VIIRS, and FY-3B MERSI (2013) (f).

make up 0.22% (183 d/a), and 4.6% of the bins are sampled more than 30.00% of the time (110 d/a). For merged products with the addition of only FY-3B MERSI, the median and maximum sampling frequencies improved to 17.30% (63 d/a) and 77.70% (283 d/a). Bins with data more than 50.00% of the time constitute 7.60% (183 d/a), and 17.40% of the bins are sampled more than 30.00% of the time (110 d/a). The results reveal obvious improvement in temporal coverage when FY-3 MERSI is included in the merger.

4.3 *Validation against in situ measurements*

Comparison with *in situ* measurements is an important means of validating the quality of satellite products, although this method may be questionable because of scarce *in situ* measurements for some products (Maritorena, 2010). The *in situ* data used herein are from a pre-existing dataset of *in situ* marine bio-optical observations, SeaBASS (Werdell and Bailey, 2002) for 2011–2013. The close spatial (3×3 pixels) and temporal (satellite and *in situ* data collected within 3 to 6 hours) windows typically used in level-2 data at 1-km resolution are not suitable for the merged products presented here, because of coarse resolution (9 km) and sparse *in situ* data. It is necessary to relax the spatial and temporal constraints to obtain the maximum number of matching points. Here, such points were considered valid when the coordinate of an *in situ* measurement was within the boundary of a merged product bin and that bin had a valid value on the same date.

Matching points were produced for the merged Chl *a* products from MERIS, MODIS, VIIRS and FY-3 MERSI, and for Chl *a* products merged using the three sensors except for FY-3 MERSI. This was done to check whether the merger with FY-3 data addition degraded product quality. Figure 9 shows matching statistics between *in situ* measurement and the satellite products. Overall, adding FY-3 MERSI to the merged Chl *a* products did not degrade the results.

4.4 *Temporal variability over 3-year period*

Time series of monthly geometric mean Chl *a* concentration from the merged products with and without FY-3, and from the individual sensors, are shown for (1) the global deep ocean (water depth greater than 1 000 m to ignore coastal waters) between latitudes 40°N and 40°S (Fig. 10), (2) northwest Pacific Ocean (NPO), and Mediterranean Sea (MS).

For global Chl *a* concentration, good agreement was found between the merged products and individual sensors for 2011–2013, with slight seasonal characteristics of two Chl *a* peaks, during early boreal spring and end of summer. Average relative deviation between the merged products with and without FY-3 is 4.1% during that period except for May, June and July of 2012 and 2013 (winter in the Southern Hemisphere). At that time, FY-3 has relatively high Chl *a* concentration compared with MODIS and VIIRS. Figure 11 shows monthly merged Chl *a* products of FY-3 MERSI and VIIRS from July 2012. The major difference between 40°N and 40°S in these two images is within the Southern Hemisphere westerly belt (around 35°–65°S). In this belt, there are strong winds and large waves throughout the year, but these become even more pronounced in winter (May, June and July). Estep and Arnone (1994) found that whitecaps and bubbles formed directly by wind-wave breaking have a clear influence on the extraction accuracy of Chl *a* concentration. The error is greater than 10%, 40% and 80% for wind speeds of 15, 20 and 25 m/s, respectively. At higher latitudes, especially in the Southern Hemisphere Rrs(443)/ Rrs(565), Rrs(490)/ Rrs(565) and

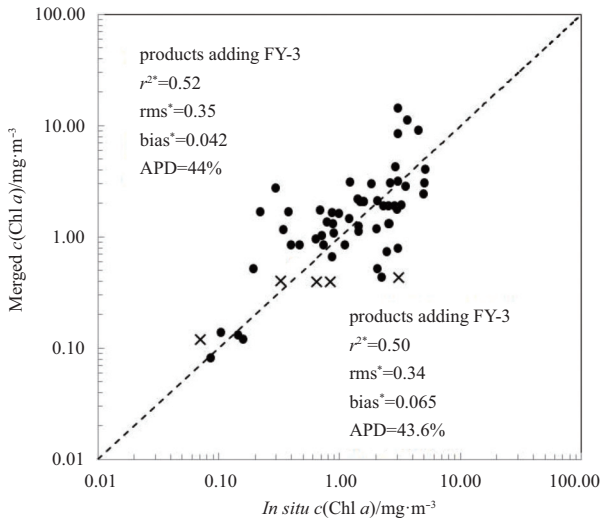

Fig. 9. Matchup statistics for the merged Chl *a* products (black dots: products without FY-3 MERSI; crosses: FY-3 MERSI products after correction, black dots plus crosses stand for the matchups of the merged products adding FY-3 MERSI; *means that the statistical measures are made based on the logarithm of Chl *a* concentration value).

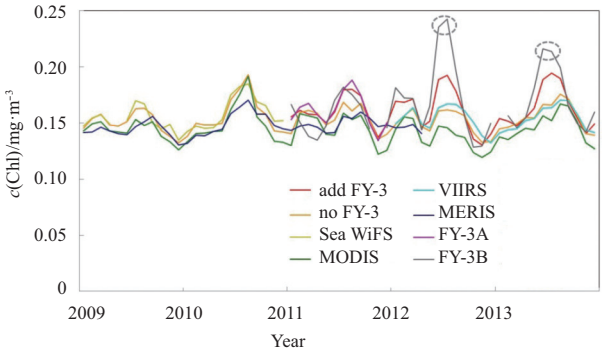

Fig. 10. Time series of global geometric mean Chl *a* (40°N–40°S, water depth greater than 1 000 m) for SeaWiFS-only, MODIS-only, MERIS-only, VIIRS-only, FY-3-only, and merged products with and without FY-3.

CI of FY-3 had strong deviations from MODIS values, causing inaccurate modification of the FY-3 data and overestimated Chl *a* concentration (Fig. 12).

For regional Chl *a* concentration, the merged products and individual sensors show good performance, consistent with clear seasonal signals in the Northwest Pacific Ocean (Fig. 13a) and Mediterranean Sea (Fig. 13b). Average relative deviations between the merged products during 2011–2013 with and without FY-3 are 4.3% and 5.8% for the NPO and MS, respectively.

4.5 *Comparison with GlobColour and MEaSUREs product sets*

Another way to assess and validate the quality of the merged product is to compare with other merged datasets. Here, the merged datasets were obtained from the MEaSUREs and GlobColour initiatives. Two Chl *a* concentration datasets were produced for GlobColour using different merging technologies, the weighted average (AVW) and Garver-Siegel-Maritorena (GSM).

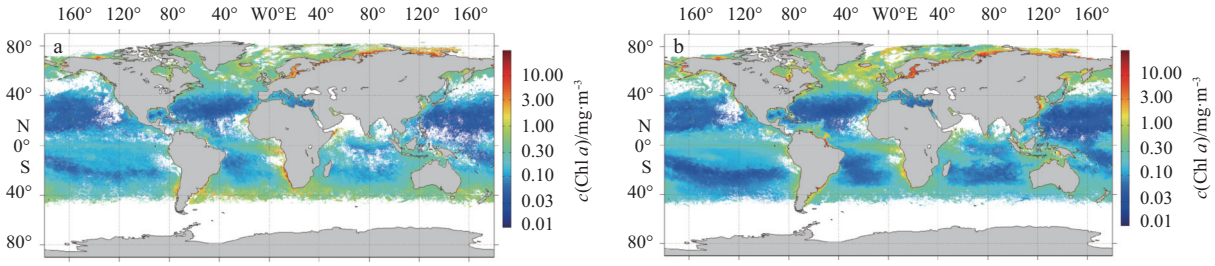

Fig. 11. Monthly global Chl *a* concentration data of July, 2012 for FY-3B (a) and VIIRS (b).

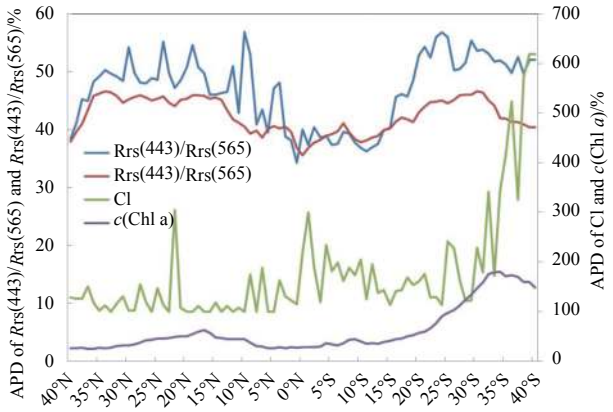

Fig. 12. Difference of Rrs(443)/Rrs(565), Rrs(490)/Rrs(565), CI and *c*(Chl *a*) retrievals between FY-3B and MODIS during May, June and July 2012.

The MEaSUREs Chl *a* concentration product was also calculated by the GSM algorithm. Table 8 shows the consistency of the present merged daily Chl *a* concentration products with GlobColour and MEaSUREs merged data from 2011. The GlobColour Chl *a* concentration merged data were generated using averaging methods and the GSM model, and MEaSUREs merged data using just the latter model. For Chl *a* concentration values of global ocean, there is a strong relationship between the merged products with FY-3 MERSI and GlobColour and MEaSUREs merged data, although the Chl *a* concentration retrieval algorithms used are different. Correlation coefficient and the APD_median are about 0.9 and 10%, respectively, similar to the consistency between GlobColour and MEaSUREs merged data, both from the GSM model.

Figure 14 shows the global distribution of the relative difference ((*x*-*y*)/*y*) between the merged data with FY-3 MERSI and GlobColour merged data from the GSM. About 87.7% bins of the global ocean (80°N–80°S) are very consistent between these two merged datasets, with an absolute relative difference less than 10%. The MS has the largest difference. Bricaud et al. (2002), Claustre et al. (2002), and D'Ortenzio et al. (2002) demonstrated that the standard NASA Chl *a* retrieval algorithms significantly overestimate the satellite Chl *a* concentration (greater than 70%) for the regions where Chl *a* concentration is less than 0.2 mg/m^3 in the MS. Inaccurate individual estimates over that sea results in the relatively large difference between the two merged data sources.

5 Conclusions

Previous works have illustrated that combining or merging data from multiple satellites can improve daily coverage of the

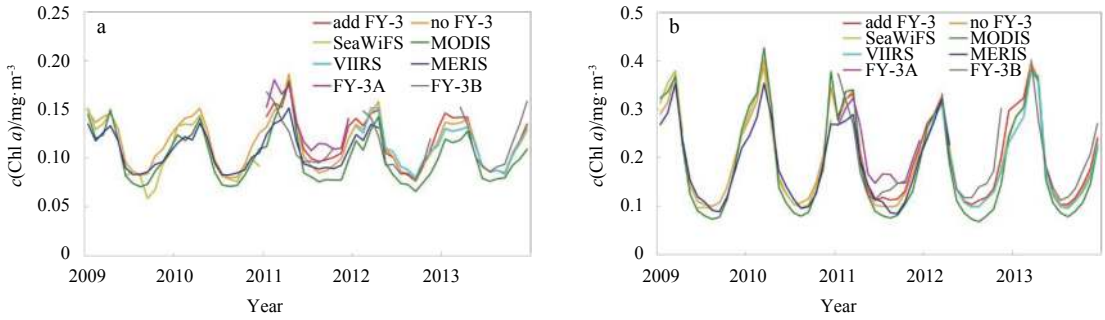

Fig. 13. Time series of regional geometric mean Chl *a* of NPO (a) and MS (b) for SeaWiFS-only, MODIS-only, MERIS-only, VIIRS-only, FY-3-only and merged products with and without FY-3.

Table 8. Consistencies of present merged monthly Chl *a* concentration products with GlobColour and MEaSUREs merged data. Statistical measures are based on logarithmic Chl *a* concentration values

	*r**	RMSE*	Bias*	APD-median*/%
With GlobColour (averaging method)	0.95	0.19	0.058	11.34
With GlobColour (GSM)	0.92	0.17	–0.002	8.91
With MEaSUREs (GSM)	0.88	0.21	0.062	8.85
GlobColour (GSM) & MEaSUREs (GSM)	0.97	0.13	–0.072	7.30

Note: *means that the statistical measures are made based on the logarithm of Chl *a* concentration value.

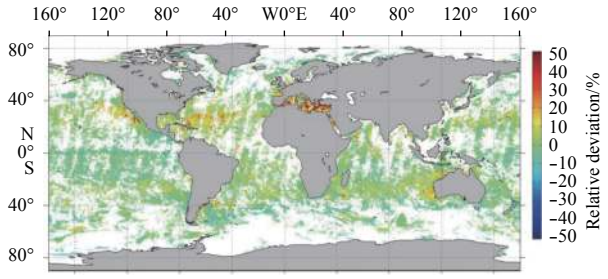

Fig. 14. Global distribution of relative difference between merged data with FY-3 MERSI and GlobColour merged data.

global ocean, which has enhanced ocean-color science (Gregg et al., 1998, Gregg and Woodward, 1998; IOCCG, 1999). The main objective here was to illustrate the importance and potential of ocean-color sensor MERSI onboard the FY-3 weather satellite for merged satellite ocean color products, taking Chl *a* concentration products as an example. The merger begins with Rrs level-3 products, and the Chl *a* concentration inversion algorithm used is a combination of CIA and OC3 proposed by Hu et al. (2012). Although the available GSM model has been documented in previous papers and was used to generate the GlobColour and MEaSUREs merged data, we did not use this approach because of poor consistency between FY-3 Rrs and MODIS Rrs data.

Generating uniform data from different data sources requires strong consistency between their datasets, within their own uncertainty levels. Other works have emphasized the consistency of Rrs products from SeaWiFS, MERIS, MODIS and VIIRS. Therefore, in this paper, much attention was given to the assessment of FY-3 MERSI Rrs data. The results show unsatisfactory agreement between FY-3 MERSI and MODIS Rrs data, which does not favor the addition of FY-3 MERSI to merged ocean-color data. However, for Chl *a* retrievals, the result is not so unfavorable. Three indices used in our Chl *a* concentration inversion algorithm, Rrs(443)/ Rrs(565), Rrs(490)/ Rrs(565) and CI of FY-3 MERSI, showed strong correlation with MODIS, with their differences mainly caused by systematic bias. Based on such relationships, the three indices can be corrected using MODIS data. After this process, the Chl *a* concentration retrievals from FY-3 MERSI showed good agreement with those from MODIS. Various error sources, such as calibration, cloud mask, atmospheric correction and data processing, can produce major differences between FY-3 MERSI and MODIS Rrs data. It is beyond the scope of the present work to analyze the contributions of these error sources.

The merged uniform ocean-color products have various potential benefits for research into marine biogeochemistry, the biosphere, or global climate change. Here, we showed spatial and temporal coverage improvements of the merged Chl *a* products with FY-3 MERSI relative to those products without FY-3 MERSI. The increase in coverage was ~9% when FY-3A and FY-3B were both added in the merger, and approximately 4.5% when only one or the other was added. By adding FY-3 MERSI to the merged Chl *a* concentration data, sampling frequency was greatly improved, with the median frequency increasing from 15.60% (approximately 57 d/a) to 29.90% (approximately 109 d/a). For the merged products without FY-3 MERSI, only 0.10% of the global ocean bins had data more than 50.00% of the time (approximately 183 d/a), but this improved to 15.50% (approximately 183 d/a) when FY-3 MERSI was added.

The merged Chl *a* concentration products were validated by comparing them with merged products lacking FY-3 and GlobColour and MEaSUREs merged data. Chl *a* concentration global geometric means between the merged products with and without FY-3 MERSI show good agreement for 2011–2013. There is also a strong relationship between the present merged data and those of GlobColour and MEaSUREs, despite their different Chl *a* concentration retrieval algorithms.

The importance and potential of FY-3 MERSI for the merged ocean-color data products were highlighted here, but there are still some issues because of poor agreement of their Rrs data with those of MODIS. In the future, there will be a focus on analyzing the error sources causing the differences between the data of these two instruments and developing correction technologies for Rrs data.

Acknowledgements

The SeaWiFS, MODIS and VIIRS data were available courtesy of NASA, and MERIS data were provided by the ESA. The authors also thank the National Satellite Meteorological Center of the China Meteorological Administration for the FY-3 MERSI data.

References

Antoine D, d'Ortenzio F, Hooker S B, et al. 2008. Assessment of uncertainty in the ocean reflectance determined by three satellite ocean color sensors (MERIS, SeaWiFS and MODIS-A) at an offshore site in the Mediterranean Sea (BOUSSOLE project). Journal of Geophysical Research, 113(C7): C07013

Antoine D, Morel A, Gordon H R, et al. 2005. Bridging ocean color observations of the 1980s and 2000s in search of long-term trends. Journal of Geophysical Research: Oceans, 110(C6): C06009, doi: 10.1029/2004JC002620

Arrigo K R, Van Dijken G L, Bushinsky S. 2008. Primary production in the Southern Ocean, 1997-2006. Journal of Geophysical Research: Oceans, 113(C8): C08004

Bailey S W, Werdell P J. 2006. A multi-sensor approach for the on-orbit validation of ocean color satellite data products. Remote Sensing of Environment, 102(1-2): 12–23

Bricaud A, Bosc E, Antoine D. 2002. Algal biomass and sea surface temperature in the Mediterranean Basin: intercomparison of data from various satellite sensors, and implications for primary production estimates. Remote Sensing of Environment, 81(2-3): 163–178

Chavez F P, Messié M, Pennington J T. 2011. Marine primary production in relation to climate variability and change. Annual Review of Marine Science, 3: 227–260

Claustre H, Morel A, Hooker S B, et al. 2002. Is desert dust making oligotrophic waters greener?. Geophysical Research Letters, 29(10): 1469

Donlon C, Berruti B, Buongiorno A, et al. 2012. The global monitoring for environment and security (GMES) Sentinel-3 mission. Remote Sensing of Environment, 120: 37–57

D'Ortenzio F, Marullo S, Ragni M, et al. 2002. Validation of empirical SeaWiFS algorithms for chlorophyll *a* retrieval in the Mediterranean Sea: a case study for oligotrophic seas. Remote Sensing of Environment, 82(1): 79–94

Estep L, Arnone R. 1994. Effect of whitecaps on determination of chlorophyll *a* concentration from satellite data. Remote Sensing of Environment, 50(3): 328–334

Fargion G S, McClain C R. 2003. MODIS Validation, Data Merger and Other Activities Accomplished by the SIMBIOS Project: 2002–2003. Greenbelt, USA: NASA/GSFC

Ford D, Barciela R. 2017. Global marine biogeochemical reanalyses assimilating two different sets of merged ocean colour products. Remote Sensing of Environment, 203(15): 40–54

Franz B A. 2003. A long-term intercomparison of oceanic optical property retrievals from MODIS-Terra and SeaWiFS in MODIS Validation, Data Merger, and Other Activities Accomplished by SIMBIOS Project: 2002–2003. Greenbelt, USA: NASA Goddard Space Flight Center

Garver S A, Siegel D A. 1997. Inherent optical property inversion of ocean color spectra and its biogeochemical interpretation: 1. Time series from the Sargasso Sea. Journal of Geophysical Research: Oceans, 102(C8): 18607–18625

Gregg W W, Conkright M E. 2001. Global seasonal climatologies of ocean chlorophyll *a* blending in situ and satellite data for the Coastal Zone color Scanner era. Journal of Geophysical Research: Oceans, 106(C2): 2499–2515

Gregg W W, Conkright M E, O'Reilly J E. et al. 2002. NOAA-NASA coastal zone color scanner reanalysis effort. Applied Optics, 41(9): 1615–1628

Gregg W W, Esaias W E, Feldman G C, et al. 1998. Coverage opportunities for global ocean color in a multimission era. IEEE Transactions on Geoscience and Remote Sensing, 36(5): 1620–1627

Gregg W W, Woodward R H. 1998. Improvements in coverage frequency of ocean color: combining data from SeaWiFS and MODIS. IEEE Transactions on Geoscience and Remote Sensing, 36(4): 1350–1353

Hlaing S, Harmel T, Gilerson A, et al. 2013. Evaluation of the VIIRS ocean color monitoring performance in coastal regions. Remote Sensing of Environment, 139: 398–414

Hooker S B, Maritorena S. 2000. An evaluation of oceanographic radiometers and deployment methodologies. Journal of Atmospheric and Oceanic Technology, 17(6): 811–830

Hu Chuanmin, Lee Zhongping, Franz B. 2012. Chlorophyll *a* aalgorithms for oligotrophic oceans: a novel approach based on three-band reflectance difference. Journal of Geophysical Research: Oceans, 117(C1): C01011, doi: 10.1029/2011JC007395

Hu Chuanmin, Feng Lian, Lee Zhongping. 2013. Uncertainties of SeaWiFS and MODIS remote sensing reflectance: implications from clear water measurements. Remote Sensing of Environment, 133: 168–182

Hu Xiuqing, Liu Jingjing, Sun Ling, et al. 2010. Characterization of CRCS Dunhuang test site and vicarious calibration utilization for Fengyun (FY) series sensors. Canadian Journal of Remote Sensing, 36(5): 566–582

IOCCG. 2007. Ocean-colour data merging. In: Gregg W, ed. Reports of the International Ocean-Colour Coordinating Group. No.6, IOCCG. Dartmouth, Canada

Johnson K S, Berelson W M, Boss E S, et al. 2009. Observing biogeochemical cycles at global scales with profiling floats and gliders: prospects for a global array. Oceanography, 22(3): 216–225

Kahru M, Jacox M G, Lee Z, et al. 2015. Optimized multi-satellite merger of primary production estimates in the California Current using inherent optical properties. Journal of Marine Systems, 147: 94–102

Kahru M, Kudela R M, Manzano-Sarabia M, et al. 2012. Trends in the surface chlorophyll *a* of the California Current: merging data from multiple ocean color satellites. Deep Sea Research Part Ⅱ: Topical Studies in Oceanography, 77-80: 89–98

Kara A B, Hurlburt H E, Rochford P A, et al. 2004. The impact of water turbidity on interannual sea surface temperature simulations in a layered global ocean model. Journal of Physical Oceanography, 34(2): 345–359

Kwiatkowska, E J. 2003. Comparisons of daily global ocean color data sets: MODIS-Terra/Aqua and SeaWiFS," in MODIS Validation, Data Merger, and Other Activities Accomplished by SIMBIOS Project: 2002–2003. Greenbelt, USA: NASA Goddard Space Flight Center

Kwiatkowska E J, Fargion G S. 2002a. Merger of ocean color information from multiple satellite missions under the NASA SIMBIOS Project Office. International Conference on Information Fusion, 1, 291-298

Kwiatkowska E J, Fargion G S. 2003a. Merger of ocean color data from multiple satellite missions within the SIMBIOS project. Proceedings of the SPIE symp. Remote Sensing of the Atmosphere, Ocean, Environment, and Space Ocean Remote Sensing and Applications. Hangzhou: SPIE, 4892: 168–182

Kwiatkowska E J, Fargion G S. 2003b. Application of machine-learning techniques toward the creation of a consistent and calibrated global Chlorophyll *a* concentration baseline dataset using remotely sensed ocean color data. IEEE Transactions on Geoscience and Remote Sensing, 41(12): 2844–2860

Le Chengfeng, Hu Chuanmin, English D, et al. 2013. Towards a long-term Chlorophyll *a* data record in a turbid estuary using MODIS observations. Progress in Oceanography, 109: 90–103

Lee Zhongping, Carder K L, Arnone R A. 2002. Deriving inherent optical properties from water color: a multiband quasi-analytical algorithm for optically deep waters. Applied Optics, 41(27): 5755–5772

Lee Zhongping, Lubac B, Werdell J, et al. 2010. An update of the quasi-analytical algorithm (QAA_v5) [WWW Document]. http://www.ioccg.org/groups/Software_OCA/QAA_v5.pdf

Lee Zhongping, Shang Shaoling, Hu Chuanmin, et al. 2015. Secchi disk depth: a new theory and mechanistic model for underwater visibility. Remote Sensing of Environment, 169: 139–149

Liang Xi, Wu Lixin. 2013. Effects of solar penetration on the annual cycle of sea surface temperature in the North Pacific. Journal of Geophysical Research: Oceans, 118(6): 2793–2801

Loeb N G, Wielicki B A, Wong T, et al. 2009. Impact of data gaps on satellite broadband radiation records. Journal of Geophysical Research, 114(D1): D11109, doi: 10.1029/2008JD011183

Maritorena S, Siegel D A, Peterson A R. 2002. Optimization of a semi-analytical ocean color model for global-scale applications. Applied Optics, 41(15): 2705–2714

Mélin F, Vantrepotte V, Clerici M, et al. 2011. Multi-sensor satellite time series of optical properties and Chlorophyll *a* concentration in the Adriatic Sea. Progress in Oceanography, 91(3): 229–244

Mélin F, Zibordi G. 2007. Optically based technique for producing merged spectra of water-leaving radiances from ocean color remote sensing. Applied Optics, 46(18): 3856–3869

Mélin F, Zibordi G, Djavidnia S. 2009. Merged series of normalized water leaving radiances obtained from multiple satellite missions for the Mediterranean Sea. Advances in Space Research, 43(3): 423–437

Maritorena S, d'Andon O H F, Mangin A, et al. 2010. Merged satellite ocean color data products using a bio-optical model: characteristics, benefits and issues. Remote Sensing of Environment, 114(8): 1791–1804

Maritorena S, Siegel D A. 2005. Consistent merging of satellite ocean color data sets using a bio-optical model. Remote Sensing of Environment, 94(4): 429–440

McClain C, Esaias W, Feldman G, et al. 2002. The proposal for the NASA sensor intercalibration and merger for biological and interdisciplinary oceanic studies (SIMBIOS) program, 1995.

McClain C R. 2009. A decade of satellite ocean color observations. Annual Review of Marine Science, 1: 19–42

Mobley C D. 1994. Light and Water: Radiative Transfer in Natural Waters. New York: Academic Press

Mobley C D, Sundman L K. 2013. HydroLight 5.2 User's Guide. Bellevue, Washington: Sequoia Scientific, Inc

Morel A, Huot Y, Gentili B, et al. 2007. Examining the consistency of products derived from various ocean color sensors in open ocean (Case 1) waters in the perspective of a multi-sensor approach. Remote Sensing of Environment, 111(1): 69–88

Murtugudde R, Beauchamp J, McClain C R, et al. 2002. Effects of penetrative radiation on the upper tropical ocean circulation. Journal of Climate, 15(5): 470–486

Platt T, Sathyendranath S. 1988. Oceanic primary production: estimation by remote sensing at local and regional scales. Science, 241(4873): 1613–1620

Pottier C, Garcon V, Larnicol G, et al. 2006. Merging SeaWiFS and MODIS/Aqua ocean color data in north and equatorial Atlantic using weighted averaging and objective analysis. IEEE Transactions on Geoscience and Remote Sensing, 44(11): 3436–3451

Saulquin B, Gohin F, Garrello R. 2011. Regional objective analysis for merging high-resolution MERIS, MODIS/Aqua, and SeaWiFS chlorophyll *a* data from 1998 to 2008 on the European Atlantic shelf. IEEE Transactions on Geoscience and Remote Sensing, 49(1): 143–154

Siegel D, Yoder J. 2007. Community Letter to NASA and NOAA Regarding Concerns over NPOESS Preparatory Project VIIRS Sensor. In: NRC of the NA Space Studies Board, ed. Ensuring the Climate Record from the NPOESS and GOES-R Spacecraft: Elements of a Strategy to Recover Measurement Capabilities Lost in Program Restructuring. Washington DC: The National Academies Press, 167–169

Sun Ling, Hu Xiuqing, Guo Maohua, et al. 2012. Multi-site calibration tracking for FY-3A MERSI solar bands. IEEE Transactions on Geoscience and Remote Sensing, 50(12): 4929–4942

Sun Ling, Guo Maohua, Zhu Jianhua, et al. 2013. FY-3A/MERSI, ocean color algorithm, products and demonstrative applications. Acta Oceanologica Sinica, 32(5): 75–81

Turpie K. 2010. Visible Infrared Imaging Radiometer Suite (VIIRS) Update. Presentation to NASA Ocean Color Research Team Meeting. New Orleans, Louisiana: National Aeronautics and Space Administration

Wang Peng, Boss E S, Roesler C. 2005. Uncertainties of inherent optical properties obtained from semianalytical inversions of ocean color. Applied Optics, 44(19): 4074–4085

Werdell P J, Bailey G S, Mcclain C R. et al. 2003. The SeaWiFS bio-optical archive and Storage System (SeaBASS): Current Architecture and Implementation. Greenbelt, USA: NASA

Zibordi G, Berthon J F, Mélin F, et al. 2009. Validation of satellite ocean color primary products at optically complex coastal sites: northern Adriatic Sea, northern Baltic Proper and Gulf of Finland. Remote Sensing of Environment, 113(12): 2574–2591

Zibordi G, Mélin F, Berthon J F. 2006. Comparison of SeaWiFS, MODIS and MERIS radiometric products at a coastal site. Geophysical Research Letters, 33(6): L06617, doi: 10.1029/2006GL025778